Low concentration magnetic nanoparticle and localized magnetic centers in different materials: studies by FMR/EPR method

N. Guskos [a,b,*]

[a] Deparment of Solid State, Faculty of Physics, University of Athens,
Panepistimiopolis, 15 784 Zografou, Athens, Greece
[b] Institute of Physics, Faculty of Mechanical Engineering and Mechatronic,
Al. Piastów 17, 70-310 Szczecin, Poland
* Corresponding e-mail address: ngouskos@phys.uoa.gr

Materials

ABSTRACT

Purpose: The aim of this review is recapitulating the temperature dependence of FMR/EPR spectra of low concentration of magnetic nanoparticles and ultralow concentration localized magnetic centers (defects, free radicals, the lower oxidation state of titanium ions) in different materials.

Design/methodology/approach: Reorientation processes correlated and isolated spin systems during changing temperature could inform about physical properties of the materials. The FMR/EPR is very usefully method for characterization novel materials as polymers/copolymers, nanotubes, TiN, TiC, Ti-Si-C-N, TiO_2, Me-Fe-V-O, $nFe_2O_3/(1-n)ZnO$ or an extended free radicals networks.

Findings: The intense almost symmetrical FMR resonance line of low concentration of magnetic nanoparticles are observed which essential are changed at different temperatures. The EPR spectra of low concentration localized magnetic nanoparticles is shown that the relaxation processes are different than for magnetic nanoparticles embed in polymer matrixes. A very low concentration of magnetic nanoparticles and localized magnetic moments could modify its physical properties (magnetic, conductivity or mechanical).

Research limitations/implications: Composite systems containing magnetic nanoparticles and localized magnetic moments promise the potential for high-density data storage, biomedical applications, catalysis, building materials, photovoltaic, metallurgy and nanotechnology sensor materialisation, among other envisaged utilisations.

Originality/value: Continue attempting to decipher the mystery and fruitfulness of magnetic nanoparticle and localized magnetic nanoparticles distributions.

Keywords: Metallic alloys; Nanoparticles; Magnetic materials; Localized magnetic moments

1. Introduction

Low concentration magnetic nanoparticles in composite materials are the subject of intensive research due to their potential integration in a broad range of technological applications extending from high-density data storage to biomedicine [1-17]. Previously review was concerning on the study by using FMR method (ferromagnetic resonance) of different materials with low concentration of magnetic nanoparticles (α-Fe, Co, Fe_3C, γ- Fe_2O_3, Fe_3O_4) [12]. There are shown that FMR method is useful for study physical properties of the copolymers and polymers materials doped by low concentration of magnetic nanoparticles. Especially it was very effectively for investigation of critical points connected with α- β- γ- relaxation or melting points which could be modified by low concentration of magnetic nanoparticles [18,19].

The following nanocomposite systems have been to-date investigated:
a) Carbon covered magnetic nickel nanoparticles embedded in PBT-PTMO polymer [14,20].
b) Magnetic interaction in frustrated systems M-Fe-V-O [21-32].
c) Magnetic properties of nanocrystalline TiN/C, TiC/C, Ti-Si-C and Ti-Si-C-N [33-41].
d) Interaction between magnetic agglomerates and extended free radicals network studied by magnetic resonance [42-44].
e) Influence of annealing and rinsing on magnetic and photocatalytic properties of TiO_2 [45,46].
f) Magnetic and electronic properties of multiwall carbon nanotubes [47-49].
g) Ferromagnetic resonance in $nFe_2O_3/(1-n)ZnO$ nanocomposites [51-57].

Among various investigated ferromagnetic metals it is the nickel nanoparticles that have attracted much attention because they can form different crystal structures with very interesting magnetic properties, see e.g. [58-64]. Magnetic nickel nanoparticles could be very useful to be introduced into nonmagnetic matrices to study their magnetic interactions and superparamagnetic state.

Multicomponent vanadates M-Fe-V-O (M(II) = Mg, Zn, Mn, Cu, Ni and Co) exhibit very interesting physical (structural, magnetic and transport) and catalytic properties [66-74]. They belong to a group of useful catalysts used for the reaction of partial oxidation of organic compounds.

Ti-Si-C-N compounds have been widely investigated, since the understanding of their physical properties can extend their application range. One of the binary phases is titanium carbide (TiC) with electron type of conductivity, a superconducting state at low temperatures, high hardness (comparable to diamond), low thermal conductivity, and one of the highest melting points [75-87].

Organic networks derived from assemblies of organic molecules, such as the class of covalent layered organic materials resulting from the reaction of cyanuric chloridewith bridging 4,4 bipyridine units, promise applications in different areas of high technology [88-97]. It has been suggested that the free radicals could form a correlated spin system at room temperature (RT) [98].

Titanium dioxide is a very important material, intensely investigated due to its various technological applications, especially in the nanoparticles form [99-103]. Whereas mono-phase anatase photocatalytic activity is generally much greater than mono-phase rutile (due to the rutile phase higher recombination rate), it was found that especially for UV light applications the most active are photocatalysts consisting of both anatase and rutile phases [104-107].

Based on their unique mechanical, electrical and thermal properties, carbon nanotubes (CNTs) attract particular attention as filler materials for polymer reinforcement, endowing the polymer matrix their high strength and stiffness together with their thermal and electrical conductivity [109,110] Efficient dispersion and interfacial stress transfer between CNTs and the surrounding polymer are major challenges for the production of CNT reinforced nanocomposites [111,112]. Covalent attachment of chemical groups on the nanotube surface through oxidizing agents is a frequent processing step utilized to improve interfacial coupling in CNT-polymer composites [113,114] which is severely impeded by the atomically smooth CNT surfaces. However, such functionalization may modify the electronic properties of CNTs through both charge transfer and defect formation [115] and compromise the composite's performance. Static magnetization in combination with electron spin resonance (EPR) being sensitive on both the spin and orbital magnetism of the CNT rolled graphene layers have been profitably exploited to investigate the electronic properties of pristine and chemically doped CNTs together with the effects low-dimensionality [116-122].

Zinc ferrite $ZnFe_2O_4$ (ZFO) belongs to one of the most important iron oxides with very interesting magnetic properties, which are intensively investigated from theoretical and experimental points of view [123-134]. Bulk magnetic ordering occurs at low temperatures with a critical point that depends strongly on the ZFO preparation conditions. The structure of spinel ferrites is constructed by filling one-eighth of the tetrahedral sites (A) and half of the octahedral sites (B) within the *fcc* oxygen sublattice. A normal spinel corresponds to the structure with all the A sites being occupied by divalent cations (Zn(II)) and the B sites by trivalent cations (Fe(III)). In the inverse-spinel structure, the Zn(II) ions occupy half of the B sites, while the other half, as well as all the A sites, are occupied by Fe(III) ions. The bulk ZFO behaves as antiferromagnetic with a Neel temperature T_N =10.5 K, as a consequence of the antiferromagnetic superexchange interaction between Fe cations. In contrast, ZFO in the nanometric range exhibits ferromagnetic behavior below a blocking temperature T_B, as it has a mixed spinel structure in which both Zn(II) and Fe(III) cations are distributed along the A and B sites. The interaction between Fe(III) located in A and B sites is stronger due to more effective overlap of the orbitals involved in the superexchange Fe-O-Fe pathway.

The aim of this review is continuing previously work [12] of the FMR study on low concentration of magnetic nanoparticles in non-magnetic matrices and EPR investigation of ultra low concentration localized magnetic centers in different materials. The FMR/EPR investigation of magnetic nanoparticle and localized magnetic centers could be a very useful method for characterisation of different materials.

2. Experimental

Samples of Ni/C nanomaterial were prepared by carburization of nanocrystalline nickel with ethylene. At first, a solution

containing nickel (II), calcium and aluminum nitrates was used to obtain nanocrystalline nickel. A solution of 25% NH3.aq was added to obtain pH equal to 8 to precipitate metal hydroxides. The obtained deposit was washed with water, filtered and dried at 340 K. The next preparation step was calcination at 770 K for 1 h to obtain the nanocrystalline nickel precursor- nickel oxide (with a small amount of structural promoters - CaO and Al_2O_3). The role of structural promoters was to stabilize the nanocrystalline nickel structure at the elevated temperatures. The chemical composition of samples was determined using the Inductively Coupled Plasma Atomic Emission Spectroscopy (ICP-AES, JY 238 Ultrace, Jobin Yvon). Nickel precursor samples containing 0.8% CaO, 3.6% Al_2O_3 were received. A sample of 1 g of this starting material was put into a quartz crucible. The crucible was placed in a high-temperature oven and next reduced (in order to transform nickel oxide into metallic nickel) under a pure (99.999%) hydrogen flow (20 dm^3/h). The reduction process was carried out in the temperature range of 300-980 K, with the heating rate of 15 K/min. The temperature of 980 K was kept for 1 h. The mass loss due to the reduction process was about 20.5%. Next, the hydrogen was replaced by ethylene (99.9%, 20 dm^3/h). The carburization process was carried out for 1 h. Next, the oven was cooled to 570 K under a flow of argon. The mean carbon content in the prepared samples was 10.2 gC/gNi. The block copoly(ether-ester)s (PBT-block-PTMO) containing Ni/C magnetic nanoparticles (0.1 and 0.25 wt%) were synthesized by melt polycondensation of dimethyl terephtalate (DMT), buthylene glycol (BG), and poly(tetramethylene glycol) (PTMEG) in the presence of tetrabutyl orthotitanate as a catalyst and with phenol derivative IRGANOX 1010 (Ciba Geigy) as an antioxidant. The Maghemite in BG was grinded and stirred for 5 min at 20 000 rpm, and next, the dispersion was sonicated (Sonoplus - Homogenissator HD 2200) for 5 min and the procedure was repeated. The materials were dispersed for 30 min to ensure a homogeneous distribution of Ni/C nanoparticles in a glycol matrix. All substrates were introduced into the reactor, where a two-stage process of a PBT-block-PTMO synthesis proceeded with continuous mixing. Full details of the polymer nanocomposites in situ preparation have been presented previously [135].

Polycrystalline samples of $M_2FeV_3O_{11-d}$ (M(II)=Mg(II), Zn(II)) were obtained by using the solid state reaction method with a stoichiometric mixture of the Fe_2O_3, V_2O_5 oxides and 3 MCO_3. $M(OH)_2·3 H_2O$ [136]. The samples were repetitively mixed, pressed into pellet and calcinated in air at 550°C for 24 hours (twice) and than at 600 °C for 24 hours (twice).

Polycrystalline $M_3Fe_4V_6O_{24}$ (M(II)=Mg(II), Zn(II), Mn(II) and (C(II)) samples were prepared by the solid-state reaction method using a stoichiometric mixture of the ZnO, V_2O_5 and Fe_2O_3 oxides, according to the following reaction [137]: $3ZnO + 3V_2O_5 + 2Fe_2O_3 = M_3Fe_4V_6O_{24}$. The compound was respectively mixed, pressed into pellets and calcinated in air at 560°C for 20 h, 580°C for 20 h and 780°C for 20 h (twice).

The organotitanium gel precursor preparation was described in detail in [138]. The gel samples were heated in a furnace in insert and/or reactive atmospheres depending on the desired products. The heating was carried out in gas atmospheres which contained argon and/or nitrogen, hydrogen and ammonia, under the atmospheric pressure in the temperature range from 293 K to 1273 K. The reactions of the TiC and TiN phases proceeded at temperatures below 800 K during these processes. The parameters of manufacturing of TiC and TiN with or without carbon as powders are subject to the patenting procedure.

Nanocrystalline powder samples of TiC+SiC+20%C and Si_3N_4+Si(C,N)+Ti(C,N)+1%C were prepared using a non-hydrolytic sol-gel organotitanium precursor technique [139].

Cyanuric chloride was recrystallized from hexane. A layered network was prepared by condensation of cyanuric chloride with bridging paraphenylenediamine in the following way. A fine slurry of cyanuric chloride was prepared by adding a solution of 1.11 g (6.00 mmol) of cyanuric chloride in 20 ml of acetone to well stirred ice-water (30 ml). Solutions of 0.972 g (9.00 mmol) of 1,4 = phenylenediamine in 20 ml of acetone and 0.756 g $NaHCO_3$ in 10 ml of water were then added and the mixture was refluxed for 1 h. The white solid was filtered off and washed with water. The wet precipitate was divided into two parts and 0.456 g (2 mmol) of ammonium persulfate in 10 ml of water was added while stirring to one of them, dispersed in 30 ml of water. A dark blue precipitate was formed. Stirring was continued for 24 h to ensure complete oxidation, following which the solid was isolated by centrifugation, washed with water and air-dried. Similarly, the other half was oxidized using 0.820 g (2.00 mmol) of ferric nitrate. Following the addition of ferric nitrate, the mixture was stirred for 48 h. Finally, a other sample was prepared by a similar procedure but using 2.10 g (5.00 mmol) of ferric nitrate and stirring the mixture for 48 h [140].

Commercial amorphous titanium dioxide supplied by Chemical Plant "Police" S.A. (Poland) with BET surface area of 238 m^2/g was used as a pristine material (TiO_2/pristine). The crude TiO_2/pristine from sulfate technology, containing also significant amount of anatase phase and around 3.5% of rutile phase, was modified with gaseous ammonia (NH_3) as follows. A defined amount - about 20 g of water suspension of TiO_2, containing around 35% of titanium dioxide and around 8% of sulfuric acid in relative to TiO_2 content, was placed in the melting pot and introduced into the tubular furnace. Then samples were calcined in NH_3 atmosphere for 4 h. After heating the furnace was slowly cooled down to room temperature, then at room temperature rinsed with Ar for 0.25 h. Subsequently, some part of such prepared materials were rinsed with 5 dm^3 of water and then dried for 24 h in a muffle furnace [45,46].

The samples were synthesized using wet chemistry method. The mixture of zinc and iron hydroxides was obtained by an addition of 26% ammonia solution to the 20% solution of zinc nitrate (V) hexahydrate and iron(III) nitrate (V) tetrahydrate. The obtained residue was filtered, dried and calcined at 573 K for 1 h. A detailed method of preparation is described elsewhere [51,141].

The FMR/EPR spectra were recorded using a standard X-band Bruker E 500 (m = 9.5 GHz) spectrometer with magnetic field modulation of 100 kHz. The magnetic field was scaled with a NMR magnetometer. The measurements were performed In the 4-295 K temperature range using an Oxford flow cryostat.

3. Results and discussion

3.1. Ni/C PBT-block-PTMO

The PBT-block-PTMO copolymers doped by magnetic nanoparticles 0.25 wt.% and 0.1 wt.% of Ni/C have shown an

Low concentration magnetic nanoparticle and localized magnetic centers in different materials: studies...

27

interesting combination of properties, such as higher melting temperature (T_m) with lower concentration, low glass transition temperature (T_g) in both doped polymers, the greater crystallization temperature for polymers with higher concentration [19]. Similar tendency was observed in polymers doped by magnetic nanoparticles γ-Fe_2O_3 [19].

Figure 1 presents the FMR spectra of 0.25% wt nickel nanoparticle covered by carbon in PBT-block-PTMO polymer in the range temperatures. The FMR spectra is dominated by very intense and broad slightly asymmetrical resonance line similar as for magnetic nanoparticles γ-Fe_2O_3 [10,13].
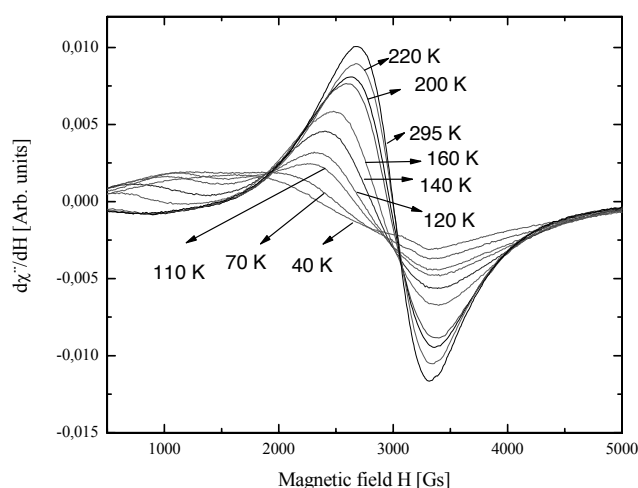

Fig. 1. Temperature dependence of the FMR spectra of 0.25 % wt Ni/C nanoparticles in PBT-block-PTMO

For analyzing FMR spectra could be used procedure proposed propose by Koksharov at al. [3,4]. The resonance line are centered is centered at g_{eff}=2.287(1) (g_{eff}=2.253(1) for 0.1%) with peak-to-peak linewidth ΔH_{pp}=69.3(2) mT (ΔH_{pp}=67.0(2) mT for 0.1%) at room temperature. The FMR resonance lines of 0.1% and 0.3% γ-Fe_2O_3 magnetic nanoparticles in polymer matrix are centered at g_{eff}=2.259(1) (ΔH_{pp}=121.3(5)) and g_{eff}=2.199(1) (ΔH_{pp}=137.7(5)), respectively [142]. The g_{eff} is connected with changing resonance conditions:

$$h\nu = g\mu_B(H_{apl} + H_{int}) \tag{1}$$

with h being Planck constant, ν is the resonance frequency, μ_B is Bohr magneton, H_{apl} *is* the externally applied magnetic field, and H_{int} the considered effective internal magnetic field which is formed by correlated spin system. The opposite behave of g_{eff} could be connected by reorientation processes where the linewidth by dipole-dipole interactions. The covered nickel ions by carbon could be caused two processes, the first decreasing concentration of magnetic nanoparticles and the second changing viscoelastic properties of materials on the localized at magnetic nanoparticles Ni/C [14]. Characteristic properties of the FMR resonance line of magnetic nanoparticls or clusters is decreasing amplitude with decreases temperatures. Owing to the analyses of the magnetic

resonance spectra registered in the 4-300 K temperature range it was possible to determine the thermal behavior of important parameters of the FMR spectra: the resonance field, the linewidth and the signal amplitude. A comparison of the studied Ni/C nanoparticles embedded into PBT-block-PTMO polymer with the previously studied maghemite nanoparticles in the multiblock poly(ether-ester) copolymer showed the presence of larger $\Delta H_r/\Delta T$ (H_r - resonance field) gradients in the former nanosystem, especially at low temperature region. This difference might be caused by different physical properties of both matrices affecting the dipole-dipole interaction between nanoparticles or agglomerates. Additional, introducing low concentration magnetic nanoparticles Ni/C in copolymer have shown that parameter $\Delta H_r/\Delta T$ essential changing in different region of temperatures than system with maghemite nanoparticles in the multiblock poly(ether-ester) copolymer [10,13,14,20].

3.2. $M_2FeV_3O_{11-d}$ and $M_3Fe_4V_6O2_{4-d}$ (M(II)=Cu(II), Zn(II), Mg(II) and Mn(II)

The both systems are constructed by multimagnetic sublattices (Fe(III) ions form two positions) [143-147]. The observed differences in site population of specific metal ions between the samples with different methods of preparation had an impact on various physical properties. Earlier this has been seen in observation of temperature dependence of the EPR spectra of these materials. It had been proposed that two processes could have an influence on the dynamical spin relaxation processes. One was assumed to be connected with the sample oxygen deficiency and the other with the distribution of the M and Fe atoms in the M(1), M(2), M(3) sites. The magnetic properties of the $M_2FeV_3O_{11-d}$ and $M_3Fe_4V_6O_{24-d}$ vanadate, characterized by a disordered distribution of diamagnetic M(II) and high-spin Fe(II) ions, are studied using electron paramagnetic resonance (EPR) measurements. Figure 2 shows representative EPR spectra of $Zn_2FeV_3O_{11-d}$ at different temperatures. A single, broad resonance line in the $g \approx 2.0$ region dominates the spectra in the whole temperature range, while a much weaker and narrow resonance line is observed at $g \approx 2.02(1)$, most probably due to paramagnetic defects. The similar is observed for both vanadate systems at room temperature. To explore the origin of the resonance line of $Zn_2FeV_3O_{11-d}$ sample, the EPR susceptibility χ(EPR) was estimated by double integration of the absorption derivative over a field range of 10 ΔHpp (peak-to-peak linewidth) at 260 K and comparison to that of weighted $CuSO_4 \cdot 5H_2O$ reference samples [144]. The value of 0.008(3) emu/mole is found for χEPR at 260 K, which corresponds to about 70% of the static susceptibility χ(260 K) = 0.0118(1) emu/mole and approximately 5.5(3) $\times$ 1020 spins/g assuming the presence of Fe(III) ions in the high-spin state ($S = 5/2$) [21]. To evaluate the temperature variation of the EPR parameters, the derivative spectra were fitted to a full Lorentz line comprising the tail of the resonance absorption at negative field, a consequence of the linearly polarized rf field that is important when the width becomes comparable to the resonance field. The integrated intensity a continuous was decreased in accordance with the Curie-Weiss law at higher temperatures with well defined peak is observed at $T \approx 55$ K for $Zn_2FeV_3O_{11-d}$, $T \approx 50$ K for $Mg_2FeV_3O_{11-d}$, $T \approx 40$ K for $Mg_3Fe_4V_6O_{24-d}$, $T \approx 40$ K for

$Zn_3Fe_4V_6O_{24-d}$ samples [21,25,28,32]. Moreover, a clearly detectable temperature variation of the *g*-factor that reaches a minimum value close to 55 K, is also observed. Such a temperature variation of the EPR parameters is frequently observed near magnetic phase transitions for ordinary antiferromagnets [149] or spin-glasses [150], due to the slowing down of spin fluctuations and the growth of internal fields.
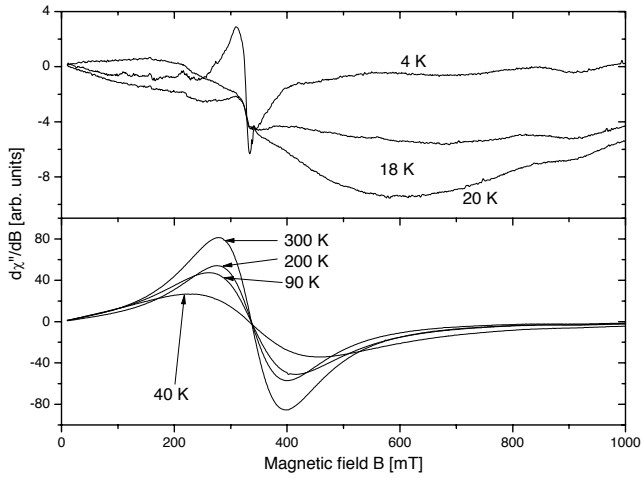

Fig. 2. The EPR spectra different temperature regions in $Zn_3Fe_4V_6O_{24}$ compound

Replacing diamagnetic ions (M(II)) with magnetic ions in $M_3Fe_4V_6O_{24-d}$ (M(II)=Cu(II) and Mn(II)) compounds could be given the magnetic interactions and relaxation processes more complicated [30,32]. Figure 3 presents the FMR spectra in $Mn_3Fe_4V_6O_{24-d}$ compounds where in lowered temperature is appeared additional resonance line arising from manganium (II) ions.
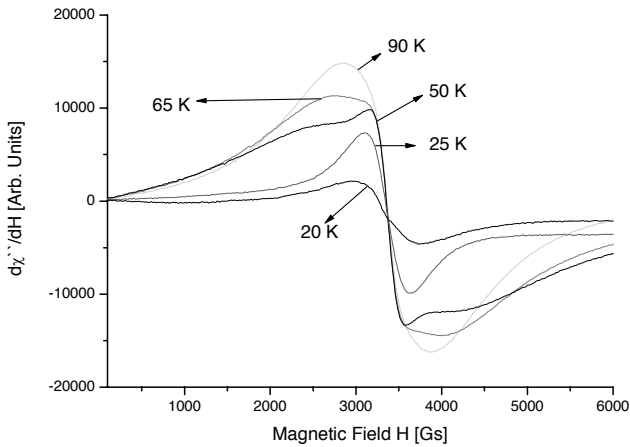

Fig. 3. The EPR spectra different temperature regions in $Mn_3Fe_4V_6O_{24}$ compound

All the samples a transition to a spin-glass-like state is observed at low temperatures, indicating appreciable spin frustration. EPR measurements verify the presence of strong aniferromagnetic coupling of the Fe(III) spins from high temperatures, while a distinct change of the temperature variation of the EPR parameters is observed at low temperatures, complying with the mean-field energy scale provided by the Curie-Weiss temperature of the system. The concomitant magnetic inhomogeneity is attributed to the presence of small amounts of oxygen deficiency that modifies the superexchange paths between magnetic Fe_2O_{10} dimeric units and leads to an inhomogeneous magnetic ground state at low temperatures.

Both the resonance field and the integrated intensity of the EPR spectrum have shown a minimum at ~220 K [24,29]. It is very surprising that replacement of different M(II) ions in the multicomponent vanadates system produces such similar behaviour in the high temperature range. Coexistence of two subsystems of magnetic iron(III) ions in the multicomponent vanadates compounds M-Fe-V-O (M(II) = Zn(II), Mg(II), Cu(II) and Mn(II)) has lead to the competition of magnetic interactions forming a frustrated system that prevented creation of an magnetic ordered state at high temperatures. It is very surprising that replacement of different M(II) ions in the multicomponent vanadates system produces such similar behaviour in the high temperature range. Replacing the M(II) ions by "strong" magnetic ions (Ni(II)) or lead ions could even lowered crystallographic structure and are given very interesting magnetic properties [27,151,152].

3.3. Nanocomposites TiN/C, TiC/C, Ti-Si-C and Ti-Si-C-N

Figure 4 displays the EPR spectra of magnetic localized centers in $TiC+SiC+20\%C$ and $Si_3N_4+Si(C,N)+Ti(C,N)+1\%C$ are taken at different temperatures. In both samples a very narrow EPR line arising from magnetic localized centers could be observed. At room temperatures a narrow line dominates the spectrum, centered at g_{eff}=2.0036(2) with peak-to-peak linewidth ΔH_{pp}=1.4(1) G and at g_{eff} =2.0029 with ΔH_{pp}=1.7(1) G in $TiC+SiC+20\%C$ and $Si_3N_4+Si(C,N)+Ti(C,N)+1\%C$ nanocomposites, respectively. The both nanocomposites in the high temperature region the line is asymmetric the best fit is obtained by using Dysonian lineshape function. In contrast, almost symmetric resonance line is recorded in the low temperature region for both samples and a good fit is made by applying Lorentzian lineshape function. Fitting of experimental spectra to Lorentzian and Dysonian lines are presented in [40]. Generally, Dysonian line consists of absorption *A* and dispersion *D* terms:

$$\frac{d\chi}{dH} = A\frac{2x}{\left(1+x^2\right)^2} + D\frac{1-x^2}{\left(1+x^2\right)^2}$$

(2)

where $x=(H-H_r)/\Delta H_{pp}$, H_r is the resonance field and ΔH_{pp} the peak-to-peak linewidth. The *D/A* ratio is connected with the

asymmetry of the resonance line. The asymmetry increases with increase in temperature indicating on the increasing role of sample conductivity [41]. For nanocomposite $Si_3N_4+Si(C,N)+Ti(C,N)+1\%C$ was recorded a more intense EPR signal than the other at room temperature while opposite is observed in the low temperature region. The thermal annealing plays a significant role in the formation of additional paramagnetic centers or could essentially change the conducting properties of materials. Dysonian lineshape of the resonance lines suggests the existence of an appreciable electric conductivity in both nanocomposites samples, much bigger in TiC+SiC+20%C.

Essential changes of EPR parameters was recorded [41]. The position of the resonance line shifts towards low magnetic fields with decreasing temperature. Similar behavior was observed for previously studied samples [40]. It could be suggested that in such a multiphase system the spin reorientation processes are more intense at low temperatures. The shift of the resonance line is the consequence of the change of the resonance condition (1). The internal magnetic field is created by the fluctuating correlated spin system. In disordered system the competition between magnetic interactions present in a spin system is an additional factor that could essentially influence the behavior of the resonance line with changing temperature. The linewidth of the resonance line increases with decrease in temperature for both samples, but the rate of this change is significant only in the low temperature range [41]. A short range magnetic order, confined to distinct spatial regions could cause the sharp variation of the EPR parameters and inhibit long-range magnetic order. Similar behaviour was observed for paramagnetic centres in quite different compounds - in ternary vanadates [25,28].

The EPR integrated intensity, defined as the area under the absorption resonance curve, is proportional to the imaginary part of the complex magnetic susceptibility. For both nanocomposite, three clear different regimes of Curie-Weiss temperature evolution could be recognized. The negative value of the Curie-Weiss temperature indicates on the presence of strong antiferromagnetic interaction while a positive value of Θ indicates on the existence of ferromagnetic interactions between the localized magnetic centers. In previously investigated samples in the high temperature range essential ferromagnetic interactions were observed [40]. The coupling of localized magnetic centers with conducting electrons could provide the domination of strong antiferromagnetic interactions at high temperatures. The competition of magnetic interactions in different sublattices prevents formation of the long-range magnetic order at high temperatures [24,29]. The presence of low temperature ferromagnetic interaction was detected in a similar material - TiC_x/C nanocomposite [35]. In order to explain the EPR results of our investigations a model of the exchange coupled two systems of localized defects and conduction electrons in the bottleneck regime could be applied [153]. A possible explanation of the observed EPR spectrum could involve electrons trapped by vacancies or defects. An argument for the electrons trapped by vacancies is that they have a g factor slightly larger than 2 and do not exhibit hyperfine structure [154,155]. Small concentration of localized magnetic centers in disordered and multiphase Ti-Si-C-N system is a very interesting subject for studying the reorientation of correlated spins and observation of their temperature evolutions. A strong antiferromagnetic interaction is observed at high temperatures while the ferromagnetic one is dominating at low temperatures. In the high temperature range the EPR spectra reflect the dominating role of conduction electrons while in the low temperature range the localized spins dominate.

3.4. Magnetic agglomerates and extended free radicals network

Figures 5 presents the temperature dependence of FMR/EPR in extended free radical network derived from condensation of cyanuric chloride with p-phenylenediamine. The measurements show the coexistence of two spectra arising from two different magnetic centers. At room temperature the narrow line centered at $g_{eff}=2.0038(1)$ with linewidth $\Delta H=7.42(2)$ Gs is assigned to free radicals, while the broader line centered at $g_{eff}=2.2536(2)$ with linewidth $\Delta H=1298(2)$ Gs is attributed to iron oxide clusters.
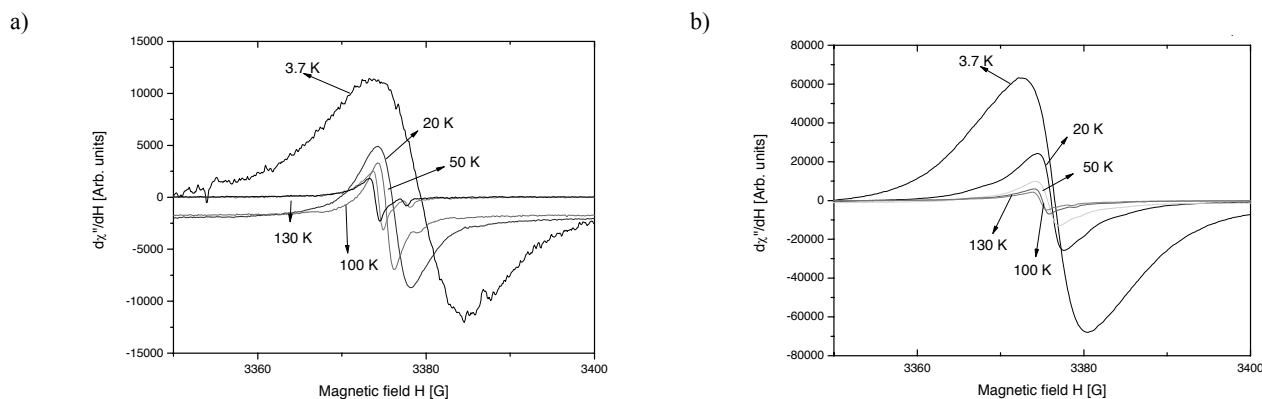
a)

b)

Fig. 4. EPR spectra of two samples from the Ti-Si-C-N system registered at different temperatures: (a) before annealing and (b) after annealing low temperature range
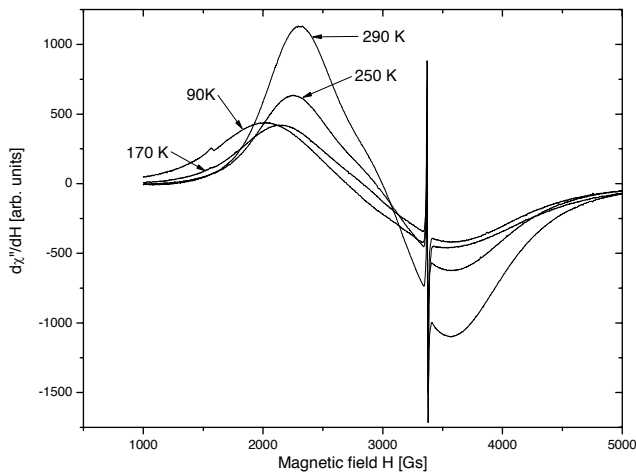
Fig. 5. EPR spectra in magnetic agglomerates and extended free radicals network derived from condensation of cyanuric chloride with p-phenylenediamine at different temperatures

For the latter, the values of the g_{eff} and linewidths are very similar behavior to what has been observed for magnetite centers at low concentration in a non-magnetic matrix [10,13]. The broad FMR line was more intense at high temperatures while the narrow line was more intense at low temperatures. The aim here is to study the interaction of magnetic clusters (or agglomerates) with free radicals. The resonance field shifts to higher magnetic fields with decreasing temperature for broad line while the opposite effect is observed for a more intense line. The broad resonance line shifts to higher magnetic field with different temperature gradients [42].

Other system with lower concentration of free radicals have been presented in [44]. The temperature dependence of the resonance field H_r and linewidth ΔH_{pp} of the broad resonance line are very similar to those reported for other nanoparticle systems in that H_r decreases and ΔH_{pp} increases with a decrease in temperature. The resonance field shifts towards low magnetic fields with the gradient $\Delta H_r/\Delta T = 2.3(2)$ G/K which is slightly greater than observed for samples with a greater concentration of magnetic nanoparticles [42,43]. The broadening of the narrow

resonance lines is more noticeable at higher temperatures for samples with magnetic agglomerates and mainly depends on their concentrations. The integrated intensity of the narrow resonance lines in both samples increases with decreasing temperature [44]. The integrated intensity essential depend from concentration of magnetic clusters. The reciprocal of the integrated intensity for the narrow lines is gone with Curie-Weiss low inn the low temperature range. The positive sign of the Curie-Weiss temperature indicates the existence of ferromagnetic interactions. The value of this parameter decreases with decreasing concentration of magnetic agglomerates [44]. A very strange behavior for the intensity of is observed in the high temperature range. At ~ 200 K a change in the type of magnetic interaction (ferromagnetic/antiferromagnetic) is observed, and is probably connected with competition of different magnetic interactions.

Small concentrations of magnetic nanoparticles embedded in a non-magnetic matrix could generate an essential internal magnetic field that might change the resonance condition (1). The dipole-dipole magnetic interaction between agglomerates and localized magnetic centers could essentially influence the reorientation processes and a large number of spins could be subjected to an average magnetic field of very low value. This behavior is very important for magnetic processes in carbons, especially for multiwall carbon nanotubes [47,48]. From the above study it is seen that large-size magnetic agglomerates at low concentration have an essential influence on all parameters FMR/EPR. The broadening of the resonance line suggests a strong dipole-dipole interaction which could have an influence on the intensity of the magnetic resonance spectra. The observed decrease in the Curie-Weiss temperature with decreasing concentration of additional magnetic centers could be an important parameter for the magnetic characterization of samples containing such centers.

3.5. Nanocomposite TiO₂

Figure 6 presents the EPR spectra of TiO_2 nanocomposite temperature at 400°C before and after rinsing with water. Before rinsing the EPR spectra have shown the presence of the resonance line of Dysononian lineshape attributed to free radicals which after rising decreasing essential.
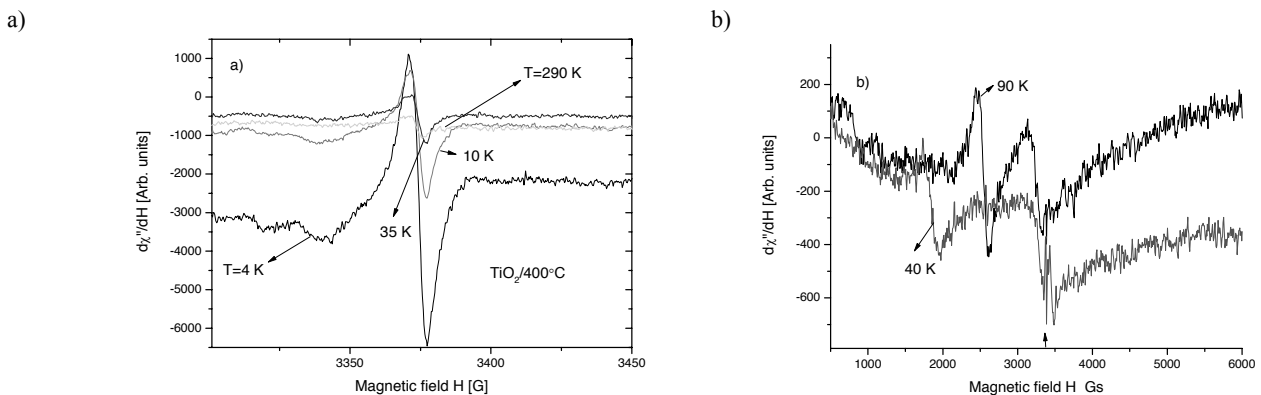
a)

b)

Fig. 6. The magnetic resonance spectra of TiO_2: before rinsing TiO_2/400°C (a) and after rinsed TiO_2/400°C (b)

The Dysonian lineshape suggests the existence of electron conductivity (skin effect) that could have an influence on the integrated intensity of the EPR spectra of free radical. The registered resonance lines were centred at g_{eff}=2.0031(4) with linewidth ΔH_{pp}=6(1) G for sample TiO_2/400°C, and g_{eff}=2.0027(4) with linewidth ΔH_{pp}=8(1) G for sample TiO_2/400°C rinsed, g_{eff}=2.0027(4) with linewidth ΔH_{pp}=5(1) G for sample TiO_2/450°C and g_{eff}=2.0032(4) with linewidth ΔH_{pp}=7(1) G for sample TiO_2/450°C rinsed which does not display any significant temperature dependence [46]. The g-factor is almost the same for all samples but the linewidth increased essentially after water rinsing in both cases. It could be suggested that the relaxation phenomena are different before and after rinsing processes. The resonance line of free radicals disappeared in the high temperature range for sample TiO_2/400°C rinsed. The character of temperature dependence of amplitude is almost the same for all samples. Samples TiO_2/400°C and TiO_2/450°C rinsed have presented the same EPR spectra but their integrated intensity was different and was about two times greater for the first sample at 4 K. The reciprocal of signal amplitude shows the Curie-type behaviour at low temperatures (below 180 K) but different dependence in the high temperature region. Probably the electron conductivity has an essential influence on the intensity of the resonance lines arising from free radicals.

For nanocomposite TiO_2/400°C rinsed additional spectra have been appeared from magnetic agglomerates and Ti(III) ions (g_{eff}=1.996(2) [46]. The temperature dependence of the amplitude due to Ti(III) ions and free radicals, the Curii-type behaviour are observed. Small concentration of magnetic nanoparticles embedded in a non-magnetic matrix produces resonance lines located in low magnetic fields. Ferromagnetically ordered states in titanium oxides as well in titanium carbide have been recorded [156,157]. The two resonance lines observed at low magnetic field are supposed to come from magnetic agglomerates. The resonance lines are shifted to lower magnetic fields with decreasing temperatures in the high temperature region. The change in resonance field is connected with the change of the resonance condition (1). It is found that more oxygen vacancies produce more recombination centers and yield more photocatalytic reactive centers improving the photocatalytic activity and the Ti(IV) ions in TiO_2 can be reduced to Ti(III) ions by reacting with reducing agent at high temperature [158,159]. Due to the upkeep of charge balance, after reduction of Ti (IV) to Ti (III) the formation of oxygen vacancies is highly possible. An increase of oxygen vacancies and trivalent titanium ions could lead to formation of the correlated spin system. For free radicals the relaxation phenomena are different before and after rinsing processes. Essential changes of EPR parameters for free radicals are observed at high temperatures and they could be connected with electron conductivity. Appeared the FMR spectra at room temperature suggested that some part of the sample could form ferromagnetic correlated spin system [45]. It could be used for application in spintronic because it is semiconductors, too.

3.6. Multiwall carbon nanotubes

The EPR spectra of the PTTPTMO/ MWNT composites consist a single resonance line with g-factor 2.0035(6), very close to the free electron value g_e=2.0023, and peak-to-peak linewidth ΔH_{pp}=5(1) G at 290 K [49]. Both ESR parameters are considerably smaller than the corresponding ones for pristine MWNTs [47,115] whose ESR spectrum is dominated by the strongly anisotropic resonance of conduction electrons. The temperature dependence of the g-factor and the resonance linewidth ΔH_{pp} of the EPR line for the PTT-PTMO/MWNT composites was comparison with the corresponding variations for the pristine MWNTs [47,49]. Both parameters vary weakly with temperature, a shallow peak can be only traced at 250 K in $\Delta H_{pp}(T)$ together with a weak broadening at $T\sim 20$ K for the MWNT polymer composites. This is in contrast with the strongly temperature dependent EPR spectra of pristine MWNTs caused by the high g-anisotropy of the CNT graphene layers. The temperature variation in the EPR parameters may generally arise from both the doping of the MWNTs as well as the introduction of a high density of paramagnetic defects prevailing in the EPR spectra of the exchange coupled system of conduction and localized spins. In the former case, the Fermi-level shift and the concomitant release of the semimetallic 2D graphite band structure diminishes the pronounced g-factor anisotropy similar to the reduction in the orbital diamagnetism, as previously observed in K and B doped MWNTs [48,118,160]. In the latter case, the formation of a large number of localized spins with spin susceptibility exceeding that of the conduction electron spin system, results in the effective reduction in the anisotropic conduction EPR spectrum of MWNTs, especially at low temperatures [122]. EPR and static magnetization measurements on composites of oxidized MWNT embedded in PTT-PTMO segmented block copolymers reveal a drastic variation in the CNT magnetic response in the polymer matrix. The diamagnetic susceptibility of the MWNTs filler and its temperature dependence is markedly reduced, suggesting the presence of effective hole-doping and substantial shift in the Fermi level, attributed to the oxygen functional groups on the oxidized CNT surface. The spin susceptibility of the composite system is considerably enhanced mainly due to the formation of a high density of paramagnetic defects, exceeding largely that of the pristine MWNTs. The temperature dependence of the corresponding ESR spectra indicates that the underlying defects are sensitive to the mechanical relaxation of the copolymer matrix, and thus to the interfaces of the oxidized MWNTs with the surrounding polymer.

3.7. nFe_2O_3/(1-n)ZnO nocomposites

The FMR spectra are dominated by intense, broad asymmetrical resonance line in the all nanocomposites at room temperatures (Fig. 7). The FMR parameters strongly depend from n and the way of preparation [50,52,55]. The registered spectra are typical for magnetic nanoparticles in a superparamagnetic phase. In such case a few different lineshapes of FMR spectra have been considered [55]. The obtained spectra have been fitted with Landau-Lifshitz line. The following equation for the Call lineshape is obtained in case of the linear polarization of the microwave field and for a perfect ferromagnet [161]:

$$I(H) = \frac{C \cdot H_r^2 \left[\left(H_r^2 + \Delta_H^2 \right) H^2 + H_r^4 \right] \Delta_H}{\left[H_r^2 \left(H - H_r \right)^2 + H^2 \Delta_H^2 \right] \left[H_r^2 \left(H + H_r \right)^2 + H^2 \Delta_H^2 \right]} \quad (3)$$

where C is a numerical constant, H_r is the resonance field, and ΔH is the linewidth. The fitting was good except and the resonance line is centered at about g_{eff}=1.998(1) with a linewidth varying in the 150-440 G range [161].
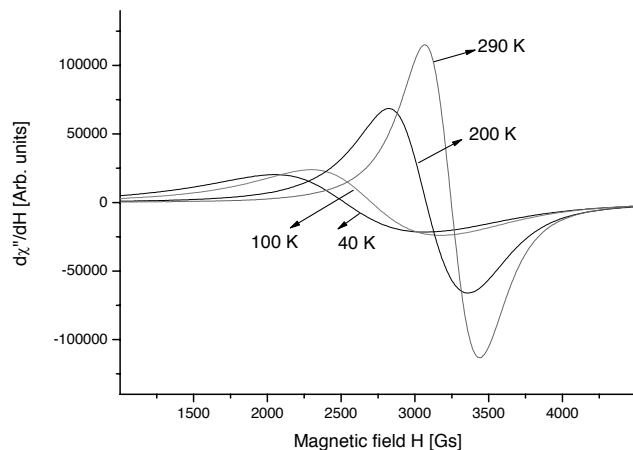

Fig. 7. The FMR spectra at different temperatures in 0.80(Fe_2O_3)/0.20ZnO

Figure 7 presents the FMR spectra in 0.80(Fe_2O_3)/0.20ZnO. The apparent amplitude of the line decreases with temperature decrease from room temperature (RT). The line shifts towards lower magnetic fields, and its linewidth increases. The apparent resonance field is defined as the magnetic field at which the first derivative absorption line changes sign, and the apparent linewidth is the doubled magnetic field difference between the resonance field and the magnetic field at which the derivative reaches a minimum. As can be seen in [54,56,57], the apparent resonance field decreases with decrease in temperature, but this change increases significantly below 40 K. An apparent linewidth increases with temperature decrease from RT in the whole investigated temperature range, but that change seems to be particularly strong in the 16-8 K range. Both the apparent resonance field and linewidth temperature dependencies are typical of observations earlier in similar nanoparticles systems in the superparamagnetic phase. The blocking temperature appears to be below 50 K. In a wide temperature range 50-290 K, the FMR spectrum of ZFO nanoparticles displays typical features of the superparamagnetic phase. FMR measurements revealed the presence of a magnetic multiphase system. The FMR response was modeled by two Callen lineshape components, and the temperature dependence of the FMR parameters was studied in the 4-290K range. One component was attributed to the ferromagnetic nanoparticles with a blocking temperature of ~25 K, having a small value of the inversion parameter. The other component is produced by nanoparticles with larger inversion parameters and with a more reconstructed surface, generating various defective magnetic phases. They are responsible for the observed spin-glass-like behavior.

4. Conclusions

The FMR/EPR is a very effective method for study materials containing magnetic nanoparticles and magnetic moments localized on the atomic level. This is particularly important in nanocomposite materials, where there are many critical points. Strongly affect the dynamic behavior of the correlated spin systems and the localized magnetic centers on the critical points. It is evident that in studying a variety of materials many far-reaching conclusions can be drawn and after this the method FMR/EPR will be very effective as a chip method for characterization nanocomposites materials.

References

[1] D.E. Speliotis, Magnetic recording beyond the first 100 Years, Journal of Magnetism and Magnetic Materials 193 (1999) 29-35.

[2] E. Troc, A. Ezzir, R. Cherkaoui, C. Chaneac, M. Nogues, H. Kachkachi, D. Fiorani, A.M. Testa, J.M. Greneche, J.P. Jolivet, Surface-related properties of γ-Fe2O3 nanoparticles, Journal of Magnetism and Magnetic Materials 221 (2000) 63-79.

[3] Yu.A. Koksharov, S.P. Gubin, I.D. Kosobudsky, G.Yu. Yurkov, D.A. Pankratov, L.A. Ponomarenko, M.G. Mikheev, M. Beltran, Y. Khodorkovsky, A.M. Tishin, Electron paramagnetic resonance spectra near the spin-glass transition in iron oxide nanoparticles, Physical Review B 63 (2001) 012407.

[4] Yu.A. Koksharov, D.A. Pankratov, S.P. Gubin, I.D. Kosobudsky, M. Beltran, Y. Khodorkovsky, A.M. Tishin, Electron paramagnetic resonance of ferrite nanoparticles, Journal of Applied Physics 89 (2001) 2293-2298.

[5] X. Chen, W. Kleemann, O. Petracic, O. Sichelschmidt, S. Cardoso, P.P. Freitas, Relaxation and aging of a superferromagnetic domain state, Physical Review B 68 (2003) 054433-1-5.

[6] [5] Y. Xiaotun, X. Lingge, N.S. Choon, C.S.O. Hardy, Magnetic and electrical properties of polypyrrole-coated γ-Fe2O3 nanocomposite particles, Nanotechnology 14 (2003) 624-629.

[7] J.L. Wilson, P. Poddar, N.A. Frey, K. Mohomed, J.P. Harmon, S. Kotha, J. Wachsmuth, Synthesis and magnetic properties of polymer nanocomposites with embedded iron nanoparticles, Journal of Applied Physics 95 (2003) 1439-1443.

[8] C.T. Hsieh, J.T. Lue, Electron spin resonance studies on quantum tunneling in sinel ferrite nanoparticles, Europen Physica Journal B35 (2003) 357-364.

[9] N. Guskos, E.A. Anagnostakis, V. Likodimos, J.Typek, M. Maryniak, U. Narkiewicz, Ferromagnetic resonance and ac conductivity of a polymer composite of Fe3O4 Journal of Applied Physics 97 (2005) 0204304.

[10] N. Guskos, V. Likodimos, S. Glenis, J. Typek, M. Maryniak, Z. Roslaniec, M. Baran, R. Szymczak, D. Petridis, M. Kwiatkowska, Matrix freezing effect on the magnetic properties of γ-Fe2O3 nanoparticles dispersed in multiblock copolymer, Journal of Applied Physics 99 (2006) 084307.

[11] P. Dutta, A. Manivannan, M.S. Sechra, N. Shah, G.P. Huffman, Magnetic properties of nearly defect-free maghemite nanocrystals, Physical Review B 70 (2004) 174428.

[12] N. Guskos, E.A. Anagnostakis, A. Guskos, FMR study of magnetic nanoparticles embedded in non-magnetic matrix, Journal of Achievementes in Materials and Manufacturing Engineering 24/1 (2007) 26-35.

[13] N. Guskos, V. Likodimos, S. Glenis, M. Maryniak, M. Baran, R. Szymczak, Z. Roslaniec, M. Kwiatkowska, D. Petridis, Magnetic properties of γ-Fe$_2$O$_3$/poly(esther-ester) copolymer nanocomposites, Journal of Nanoscience and Nanotechnology 8 (2008) 2127-2134.

[14] N. Guskos, M. Maryniak, J. Typek, P. Podsiadly, U. Narkiewicz, E. Senderek, Z. Rosłaniec, Carbon covered magnetic nickel nanoparticles embedded in PBT-PTMO polymer: preparation and magnetic properties, Journal of Non-crystalline Solids 355 (2009) 1400-1404.

[15] M.R. Dudek, N. Guskos, E. Senderek, Z. Roslaniec, Temperature dependence of the FMR absorption lines in viscoelastic magnetic materials, Journal of Alloys and Compounds 504/2 (2010) 289-295.

[16] N. Guskos, J. Typek, G. Zolnierkiewicz, K. Wardal, D. Sibera, U. Narkiewicz, Magnetic resonance study of nanocrystalline ZnO nanopawders doped with Fe$_2$O$_3$ obtained by hydrothermal synthesis, Reviews on Advanced Materials Science 29 (2011) 142-149.

[17] M.R. Dudek, N. Guskos, M. Kosmider, Thermal effects on the ferromagnetic resonance in polymer composites with magnetic nanoparticles fillers in nanoparticles, Smart nanoparticles technology, A.A. Hashim (Ed.), InTech, Rijeka, 2012, 373-386.

[18] J. Majszczyk, N. Guskos, J. Typek, M. Maryniak, Z. Roslaniec, M. Kwiatkowska, D. Petridis, Low concentration of magnetic nanoparticle (γ-Fe$_2$O$_3$) effect on the interfacial polarization (MWS) and glass transition in poly(ether-b-ester) copolymer, Journal of Non-crystalline Solids 352/40-41 (2006) 4279-4282.

[19] M. Maryniak, N. Guskos, J. Typek, A. Guskos, K. Goracy, Z. Roslaniec, M. Kwiatkowska, DSC and TGA measurements at high temperatures of polymer composites with nanocrystalline γ-Fe$_2$O$_3$, Polimers 54 2009) 546.

[20] N. Guskos, J. Typek, B.V. Padlyak, Yu.K. Gorelenko, I. Pelech, U. Narkiewicz, E. Senderek, A. Guskos, Z. Roslaniec, In situ synthesis, morphology and magnetic properties poly(ether-ester) multiblock copolymer/carbon-covered nickel nanosystem, Journal of Non-Crystalline Solids 356/37-40 (2010) 1893-1901.

[21] V. Likodimos, N. Guskos, S. Glenis, R. Szymczak, A. Bezkrovnyj, M. Wabia, J. Typek, M. Kurzawa, I. Rychlowska-Himmel, A. Blonska-Tabero, Magnetic properties of the antiferromagnetic site-disordered vanadate Zn$_2$FeV$_3$O$_{11}$, Europen Physica Journal B 38 (2004) 13-19.

[22] H. Fuks, M. Wabia, J. Typek, A. Worsztynowicz, N. Guskos, M. Kurzawa, M. Bosacka, R. Szymczak, M. Baran, I. Rychlowska-Himmel, Temperature evolution of the EPR spectra in Mg$_2$CrV$_3$O$_{11-x}$ compound, Molecular Physics Reports 39 (2004) 43-49.

[23] N. Guskos, J. Typek, G. Zolnierkiewicz, A. Blonska-Tabero, M. Kurzawa, M. Bosacka, Magnetic resonance study of M$_3$Fe$_4$V$_6$O$_{24}$ (M=Mg, Zn, Mn, Cu, Co) compound, Materials Science-Poland 23/4 (2005) 923-928.

[24] G. Zolnierkiewicz, N. Guskos, J. Typek, A. Blonska-Tabero, Competing magnetic interactions in Zn$_3$Fe$_4$V$_6$O$_{24}$ studied by electron paramagnetic resonance, Acta Physica Polonica A 109/4-5 (2006) 675-679.

[25] N. Guskos, V. Likodimos, J. Typek, G. Zolnierkiewicz, R. Szymczak, A. Blonska-Tabero, Magnetic properties of the Mg$_2$FeV$_3$O$_{11-x}$ site-disordered vanadate, Journal of Non-Crystalline Solids 352/40-41 (2006) 4179-1482.

[26] G. Zolnierkiewicz, N. Guskos, J. Typek, A. Blonska-Tabero, EPR and TGA study of two Zn$_3$Fe$_4$V$_6$O$_{24-x}$ samples prepared by different thermal treatments, Journal of Non-Crystalline Solids 352/40-41 (2006) 4362-4365.

[27] N. Guskos, J. Typek, G. Zolnierkiewicz, A. Blonska-Tabero, M. Kurzawa, S. Los, W. Kempinski, Interaction thermal annealing processes on the spectroscopic properties of Ni$_2$FeV$_3$O$_{11-\delta}$ compound, Materials Science-Poland 24 (2006) 985.

[28] N. Guskos, V. Likodimos, S. Glenis, G. Zolnierkiewicz, J. Typek, R. Szymczak, A. Blonska-Tabero, Magnetic frustration in the site ordered Mg$_3$Fe$_4$(VO$_6$)$_4$ vanadate, Journal of Applied Physics 101 (2007) 103922.

[29] G. Zolnierkiewicz, N. Guskos, J. Typek, E.A. Anagnostakis, A. Blonska-Tabero, M. Bosacka, Competition of magnetic interactions in M$_3$Fe$_4$V$_6$O$_{24}$(M(II)=Zn, Cu, Mn, Mg) compounds studies by EPR at high temperatures, Journal of Alloys and Compounds 471/1-2 (2009) 28-32.

[30] N. Guskos, H. Ohta, G. Zolnierkiewicz, S. Okubo, Wei-min Zhang, J. Typek, C. Rudowicz, R. Szymczak, M. Bosacka, T. Nakamura, Magnetic interactions in frustrated Mn$_3$Fe$_4$(VO$_4$)$_6$, Journal of Non-Crystalline Solids 355 (2009) 1419-1426.

[31] G. Zolnierkiewicz, N. Guskos, J. Typek, Magnetic frustration in M-Fe-V-O system, Current Topics in Biophysics A 33 (2010) 277-281.

[32] N. Guskos, G. Zolnierkiewicz, J. Typek, R. Szymczak, A. Blonska-Tabero, Study of magnetic inhomogeneity in b-Cu$_3$Fe$_4$V$_6$O$_{24}$, Materials Science-Poland 30/1 (2012) 1-9.

[33] N. Guskos, T. Bodziony, A. Biedunkiewicz, K. Aidinis, Temperature dependence of the EPR spectra of the nanocrystalline TiN and TiC dispersed in a carbon matrix, Acta Physica Polonica A 108/2 (2005) 311-316.

[34] T. Bodziony N. Guskos, A. Biedunkiewicz, J. Typek, R. Wrobel, M. Maryniak, Characterization and EPR studies of TiC and TiN ceramics at room temperature, Materials Science-Poland 23/4 (2005) 899-907.

[35] N. Guskos, V. Likodimos, S. Glenis, G. Zolnierkiewicz, J. Typek, C.L. Lin, A. Biedunkiewicz, Magnetic properties of TiC$_x$/C nanocomposites, Journal of Non-Crystalline Solids 354/35-39 (2008) 4330-4333.

[36] N. Guskos, E.A. Anagnostakis, G. Zolnierkiewicz, V. Likodimos, J. Typek, A. Guskos, A. Biedunkiewicz, Magnetic agglomerates in the ternary nanomaterial system Ti-Si-C, Elektronika 5 (2008) 18.

[37] N. Guskos, E.A. Anagnostakis, K.A. Karkas, A. Guskos, A. Biedunkiewicz, P. Figiel, Magnetic and transport properties of nanocrystalline titanium carbide in carbon matrix, Electron transport in nanosystems, NATO Science for Peace and Security Series B, Physics and Biophysics (2008) 315-327.

[38] N. Guskos, T. Bodziony, M. Maryniak, J. Typek, A. Biedunkiewicz, Paramagnetic centers in nanocrystalline TiC/C system, Journal of Alloys and Compounds 455/1 (2008) 52-54.

[39] N. Guskos, T. Bodziony, J. Typek, G. Zolnierkiewicz, M. Maryniak, A. Biedunkiewicz, Ageing effect in nanocrystalline TiC/C studied by EPR, Journal of Alloys and Compounds 470/1-2 (2009) 51-54.

[40] N. Guskos, E.A. Anagnostakis, G. Zolnierkiewicz, J. Typek, A. Biedunkiewicz, P. Figiel, A. Guskos, K.A. Karkas, EPR study of Ti-Si-C-N system, Reviews on Advanced Materials Science 23/2 (2010) 189-195.

[41] N. Guskos, E.A. Anagnostakis, G. Zolnierkiewicz, J. Typek, A. Biedunkiewicz, A. Guskos, P. Berczynski, Effect of annealing on EPR spectra of Ti-Si-C-N samples, Materials Science-Poland 30/1 (2012) 23-31.

[42] N. Guskos, G. Zolnierkiewicz, J. Typek, A. Guskos, D. Petridis, Extended free radical network derived from condensation of cyanuric chloride with p-Phenylenediamine: EPR/FMR study, Journal of Non-Crystalline Solids 354/35 (2008) 4211-4213.

[43] N. Guskos, G. Zolnierkiewicz, J. Typek, A. Guskos, D. Petridis, Influence of concentration of free radicals/magnetic agglomerates on magnetic resonance spectrum in organic matrix, Reviews on Advanced Materials Science 23/2 (2010) 164-168.

[44] N. Guskos, G. Zolnierkiewicz, J. Typek, A. Guskos, P. Berczynski, D. Petridis, Interaction between magnetic agglomerates and extended free radicals network studied by magnetic resonance, Central European Journal of Physics 10/1 (2012) 166-171.

[45] N. Guskos, A. Guskos, J. Typek, P. Berczynski, D. Dolat, B. Grzmil, A. Morawski, Influence of annealing and rinsing on magnetic and photocatalytic properties of TiO_2, Materials Science and Engineering B 177/2 (2012) 223-227.

[46] N. Guskos, A. Guskos, G. Zolnierkiwicz, J. Typek, P. Berczynski, D. Dolat, B. Grzmil, B. Ohtani, A.W. Morawski, Spectroscopic and photocatalytic properties of N-modified TiO_2 prepared by different annealing and water-rinsing processes, Materials Chemistry and Physics, 2012.

[47] V. Likodimos, S. Glenis, N. Guskos, C.L. Lin, Magnetic and electronic properties of multiwall carbon nanotubes, Physical Review B 68 (2003) 045417.

[48] S. Glenis, V. Likodimos, N. Guskos, C.L. Lin, Magnetic properties of multiwall carbon nanotubes, Journal of Magnetism and Magnetic Materials 272-276 (2004) 1660-1661.

[49] [47] V. Likodimos, S. Glenis, N. Guskos, C.L. Lin, Antiferromagnetic behavior in single-wall carbon nanotubes, Physical Review B 76 (2007) 075420.

[50] S. Glenis, V. Likodimos, N. Guskos, D. Yaramis, G. Zolnierkiewicz, A. Szymczyk, C.L. Lin, Magnetic properties of carbon nanotube poly(ether-ester) nanocomposites, Journal of Applied Physics 108/5 (2010) 054314.

[51] D. Sibera, U. Narkiewicz, N. Guskos, G. Zołnierkiewicz, The preparation and EPR study of nanocrystalline $ZnFe_2O_4$, Journal of Physics, Conference Series 146 (2009) 1-5.

[52] N. Guskos, G. Zolnierkiewicz, J. Typek, D. Sibera, U. Narkiewicz, Magnetic resonance study of $ZnO-Fe_2O_3$-$ZnFe_2O_4$ system, Reviews on Advanced Materials Science 23 (2010) 224-228.

[53] N. Guskos, S. Glenis, G. Zolnierkiewicz, J. Typek, D. Sibera, J. Kaszewski, D. Moszyński, W. Łojkowski, U. Narkiewicz, Ferromagnetic resonance in Fe_2O_3/ZnO nanocomposites, Physica B 405/18 (2010) 4054-4058.

[54] N. Guskos, S. Glenis, G. Zolnierkiewicz, J. Typek, D. Sibera, U. Narkiewicz, FMR Study of temperature dependence of magnetic properties of nanocrystalline $0.90(Fe_2O_3)/0.10ZnO$, Acta Physica Polonica A 120/6 (2011) 1070-1073.

[55] N. Guskos, J. Typek, G. Zolnierkiewicz, K. Wardal, D. Sibera, U. Narkiewicz, Magnetic resonance study of nanocrystalline ZnO nanopawders doped with Fe_2O_3 obtained by hydrothermal synthesis, Reviews on Advanced Materials Science 29 (2011) 142-149.

[56] N. Guskos, S. Glenis, J. Typek, G. Zolnierkiewicz, P. Berczynski, K. Wardal, A. Guskos, D. Sibera, D. Moszynski, W. Lojkowski, U. Narkiewicz, Magnetic properties of $ZnFe_2O_4$ nanoparticles, Central European Journal of Physics 10 (2012) 470-477.

[57] N. Guskos, S. Glenis, G. Zolnierkiewicz, J. Typek, P. Berczynski, A. Guskos, D. Sibera, U. Narkiewicz, Magnetic properties of $ZnFe_2O_4$ ferrite nanoparticles embedded in ZnO Matrix, Applied Physics Letters 100/12 (2012) 122403.

[58] V.F. Puntes, K.M. Krishan, A.P. Alivisatos, Colloidal nanocrystal shape and size control, The case of cobalt, Science Magazine 291 (2001) 2115-2117.

[59] L.F. Yin, D.H. Wei, N. Lei, L.H. Zhou, C.S. Tian, G.S. Dong, X.F. Jin, L.P. Guo, Q.J. Jia, R.Q. Wu, Magnetocrystalline anisotropy in permalloy revisited, Physical Review Letters 97 (2006) 067203.

[60] L. He, W. Zheng, W. Zhou, H. Du, C. Chen, L. Guo, Size-dependent magnetic properties of nickel nanochains, Journal of Physics, Condensed Matter 19/3 (2007) 036216.

[61] F. Tian, J. Zhu, D. Wei, Phase transition and magnetism of Ni nanowire arrays, The Journal of Physical Chemistry C 111/19 (2007) 6994-6997.

[62] V. Srinivas, S.K. Barik, B. Bodo, D. Karmakar, T.V.C. Rao, Magnetic and electrical properties of oxygen stabilized nickel nanofibers prepared by the borohydride reduction method, Journal of Magnetism and Magnetic Materials 320/6 (2008) 788-795.

[63] P. Yu, X.F. Jin, J. Kudrnovsky, D.S. Wang, P. Bruno, Curie temperature of fcc and bcc nicle and permalloy, Supercell and Green's function methods, Physical Review B 77 (2008) 054431.

[64] T. Nagao, Y. Kubo, A. Koizumi, H. Kobayashi, M. Itou, N. Sakai, Momentum-density distribution of magnetic electrons in ferromagnetic nickel, Journal of Physics: Condensed Matter 20/5 (2008) 055201.

[65] W.D. Harding, H.H. Kung, V.L. Kozhernik, K.R. Poeppelmeier, Phase equilibria and butane oxidation studies of the $MgO-V_2O_5-MoO_3$ system, Journal of Catalysis 144 (1993) 597-610.

[66] M.A. Lafontaine, J.M. Greneche, Y. Laligant, G. Ferey, [beta]-$Cu_3Fe_4(VO_4)_6$: Structural study and relationships; physical properties, Journal of Solid State Chemistry 108/1 (1994) 1-10.

[67] S.A. Korili, S. Ruiz, B. Delmon, Oxidative dehydrogenation of n-pentane on magnesium vanadate catalysts, Catalysis Today 32/1 (1996) 229-235.

[68] X. Wang, D.A. Vander Griend, C.L. Stern, K.P. Poeppelmeir, Structure and cation distribution of new ternary vanadates $FeMg_2V_3O_{11}$ and $FeZn_2V_3O_{11}$, Journal of Alloys and Compounds 298 (2000) 119-124.

[69] P. Rybarczyk, H. Berndt, J. Radnik, M.-M. Pohl, O. Buyerskaya, M. Baerns, A. Bruckner, The structure of active sites in Me-V-O catalysts (Me = Mg, Zn, Pb) and its influence on the catalytic performance in the oxidative dehydrogenation (ODH) of propane, Journal of Catalysis 202/1 (2001) 45-58.

[70] L.E. Briand, J.-M. Jehng, L. Cornaglia, A.M. Hirt, I.E. Wachs, Quantitative determination of the number of surface active sites and the turnover frequency for methanol oxidation over bulk metal vanadates, Catalysis Today 78/1 (2003) 257-268.

[71] N. Guskos, M. Wabia, M. Kurzawa, A. Bezkrovnyj, J. Typek, I. Rychlowska-Himmel, A. Blonska-Tabero, Neutron Diffraction Study of $M_{g2}FeV_3O_{11-\delta}$, Compounds, Radiation Effects and Defects in Solids 158 (2003) 369-374.

[72] N. Guskos, J. Typek, F.A. Bezkrovnyj, V. Likodimos, M. Wabia, M. Kurzawa, E.A. Anagnostakis, G. Gasiorek, Neutron studies of cation disorder in $Zn_2FeV_3O_{11-\delta}$, Journal of Alloys and Compounds 377/1-2 (2004) 47-52.

[73] N. Guskos, A. Bezkrovnjj, J. Typek, N.Yu. Ryabova, A. Blonska-Tabero, M. Kurzawa, M. Maryniak, Neutron study of $Zn_3Fe_4V_6O_{24}$, Journal of Alloys and Compounds 391/1-2 (2005) 20-25.

[74] A. Beskrovnyy, N. Guskos, J. Typek, N.Yu. Ryabova, A. Blonska-Tabero, M. Kurzawa, G. Zolnierkiewicz, Crystal structure of $Mg_3Fe_4V_6O_{24}$ studies by neutron diffraction, Reviews on Advanced Materials Science 12 (2006) 166-171.

[75] P. Eklund, C. Virojanadara, J. Emmerlich, L.I. Johansson, H. Hogberg, L. Hultman, Photoemission studies of Ti_3SiC_2 and nanocrystalline-TiC/amorphous-SiC nanocomposite thin films, Physical Review B 74 (2006) 045417.

[76] H.O. Gulsoy, Mechanical properties of injection moulded 316L stainless steels with (TiC)N additions, Powder Metallurgy 50/3 (2007) 271-275.

[77] W.D. Leroy, C. Detavernier, R.L. van Meirhaeghe, C. Lavoiec, Thin film solid-state reactions forming carbides as contact materials for carbon-containing semiconductors, Journal of Applied Physics 101/5 (2007) 053714.

[78] J.M. Cordoba, M.J. Sayagues, M.D. Alcala, F.J.J. Gotor, Synthesis of Ti_3SiC_2 powders: Reaction mechanism, Journal- American Ceramic Society 90/3 (2007), 825-830.

[79] E.I. Isaev, S.I. Simak, I.A. Abrikosov, R. Ahuja, Y.K. Vekilov, M.I. Katsnelson MI, A.I. Lichtenstein, B. Johansson, Phonon related properties of transition metals, their carbides, and nitrides: A first-principles study, Journal of Applied Physics 101 (2007) 123519.

[80] D. Vallauri, I.C. Atias Cityplaceadrian, A. Chrysanthou, $TiC-TiB_2$ composites: A review of phase relationships, processing and properties, Journal of the European Ceramic Society 28/8 (2008) 1697-1713.

[81] L.E. Toth, Transition metal carbide and nitrides, Academic Press, New York, 1971.

[82] A.A. Rempel, Atomic and vacancy ordering in nonstoichiometric carbides, Physics-Uspekhi 39 (1996) 31-56.

[83] J. Izquirdo, A. Vega, S. Bouarab, M.A. Khan, Optical conductivity in substoichiometric titanium carbides, Physcal Review B 58/7 (1998) 3507-3510.

[84] C. Acha, M. Monteverde, M. Nunez-Regueiro, Electrical resistivity of the Ti4O(7) Magneli phase under high pressure, The European Physical Journal B 34/4 (2003) 421-428.

[85] A.I. Gusev, S.Z. Nazarova, Magnetic susceptibility of nonstoichiometric compounds of transition d-metals, Uspekhi Fizicheskikh Nauk 175/7 (2005) 681-704.

[86] E.I. Isaev, R. Ahuja, S.I. Simak, A.I. Lichtenstein, Yu.Kh. Vekilov, B. Johansson, I.A. Abrikosov, Anomalously enhanced superconductivity and ab initio lattice dynamics in transition metal carbides and nitrides, Physical Review B 72/6 (2005) 064515.

[87] A.L. Ivanovskii, Magnetic effects induced by sp impurities and defects in nonmagnetic sp materials, Physics-Uspekhi 50/10 (2007) 1031.

[88] W.J. Bae, K.H. Kim, W.H. Jo, Y.H. Park, A water-soluble and self-doped conducting polypyrrole graft copolymer, Macromolecules 38/4 (2005) 1044-1047.

[89] J.P. Majoral, A. M. Caminade, Dendrimers Containing heteroatoms (Si, P, B, Ge, or Bi), Chemical Reviews 99 (1999) 845-880.

[90] A.B. Bourlinos P. Dallas, Y. Sanakis, D. Stamopoulos, C. Trapalis, D. Niarchos, Synthesis and characterization of a pi-conjugate, covalent layered network derived from condensation polymerization of the 4,4 '-bipyridine-cyanuric chloride couple, European Polymer Journal 42/11 (2006) 2940-2948.

[91] G. Blotny, Recent applications of 2,4,6-trichloro-1,3,5-triazine and its derivatives in organic synthesis, Tetrahedron 62/41 (2006) 9507-9522.

[92] M. Shahid, R.S. Ashraf, E. Klemm, S. Sensfuss, Synthesis and properties of novel low-band-gap thienopyrazine-based poly(heteroarylenevinylene)s, Macromolecules 39 (2006) 7844-7853.

[93] R.Y.C. Shin, T. Kietzke, S. Sudhakar, A. Dodabalapur, Z. K. Chen, A. Sellinger, N-type conjugated materials based on 2-vinyl-4,5-dicyanoimidazoles and their use in solar cells, Chemistry of Materials 19/8 (2007) 1892-1894.

[94] H.K.C. Pandya, Z.I. Niazimbetova, F.L. Beyer, M.E. Galvin, Role of symmetry and charge delocalization in two-dimensional conjugated molecules for optoelectronic applications, Chemistry of Materials 19/5 (2007) 993-1001.

[95] P. Dallas, A.B. Bourlinos, D. Petridis, N. Boukos, K. Papadokostaki, D. Niarchos, N. Guskos, Synthesis and characterization of 2-D and 3-D covalent networks derived from triazine central cores and bridging aromatic diamines, Polymer 49/5 (2008) 1137-1144.

[96] P. Dallas, D. Stamopoulos, N. Boukos, V. Tzitzios, D. Niarchos, D. Petridis, Characterization, magnetic and transport properties of polyaniline synthesized through interfacial polymerization, Polymer 48/11 (2007) 3162-3169.

[97] P. Dallas, D. Niarchos, D. Vrbanic, N. Boukos, S. Pejovnik, C. Trapalis, D. Petridis, Interfacial polymerization of pyrrole and in situ synthesis of polypyrrole/silver nanocomposites, Polymer 48/7 (2007) 2007-2013.

[98] A.B. Bourlinos, V. Georgakilas, V. Tzitzios, N. Boukos, R. Herrera, E.R. Giannelis, Functionalized carbon nanotubes: Synthesis of meltable and amphiphilic derivatives, Small 2/10 (2006) 1188-1191.

[99] A. Fernandez, G. Lassaletta, V. M. Jimenez, A. Justo, A.R. GonzalezElipe, J.M. Herrmann, H. Tahiri, Y. AitIchou, Preparation and characterization of TiO2 photocatalysts supported on various rigid supports (glass, quartz and stainless steel), Comparative studies of photocatalytic activity in water purification, Applied Catalysis B, Environmental 7/1 (1995) 49-63.

[100] K.D. Schierbaum, U.K. Kirner, J.F. Geiger, W. Göpel, Conductance, work function and catalytic activity of SnO2-based gas sensors, Sensors and Actuators B, Chemical 3/3 (1991) 205-214.

[101] A.L. Linsebigler, G. Lu, J.T. Yates, Jr., Photocatalysis on TiO2 surfaces: principles, mechanisms, and selected results, Chemical Reviews 95 (1995) 735-758.

[102] D.B. Strukov, G.S. Sneider, D.R. Stewart, R.S. Williams, The missing memristor found, Nature 453 (2008) 80-83.

[103] R. Waser, R. Dittmann, G. Staikov, K. Szot, Redox-based resistive switching memories - nanoionic mechanisms, prospects, and challenges, Advanced Materials 21/25-26 (2009) 2632-2663.

[104] U. Stafford, K.A. Gray, P.V. Kamat, V. Arvind, An in situ diffuse reflectance FTIR investigation of photocatalytic degradation of 4-chlorophenol on a TiO2 powder surface, Chemical Physics Letter 205 (1993) 55-61.

[105] G. Riegel, J.R. Bolton, Photocatalytic efficiency variability in TiO2 particles, The Journal of Physical Chemistry 99 (1995) 4215-4224.

[106] R.R. Bacsa, J. Kiwi, Effect of rutile phase on the photocatalytic properties of nanocrystalline titania during the degradation of p-coumaric acid, Applied Catalysis B, Environmental 16/1 (1998) 19-29.

[107] G. Colon, M.C. Hidalgo, J.A. Navio, Photocatalytic deactivation of commercial TiO2 samples during simultaneous photoreduction of Cr(VI) and photooxidation of salicylic acid, Journal of Photochemistry and Photobiology A, Chemistry 138 (2001) 79-85.

[108] M. Endo, M.S. Strano, P.M. Ajayan, Potential applications of carbon nanotubes, Topics in Applied Physics 111 (2008) 13-62.

[109] J.N. Coleman, U. Khan, W.J. Blau, Y.K. Gun'ko, Small but strong, A review of the mechanical properties of carbon nanotube-polymer composites, Carbon 44/9 (2006) 1624-1652.

[110] Y.Y. Huang, S.V. Ahir, E.M. Terentjev, Infrared actuation in aligned polymer-nanotube composites, Physical Review B 73 (2006) 125422.

[111] P.M. Ajayan, J.M. Tour, Materials science - nanotube composites, Nature 447 (2007) 1066-1068.

[112] L. Vaisman, G. Marom, H.D. Wagner, Dispersions of surface-modified carbon nanotubes in water-soluble and water-insoluble polymers, Advanced Functional Materials 16 (2006) 357-363.

[113] F.H. Gojny, J. Nastalczyk, Z. Roslaniec, K. Schulte, Surface modified multi-walled carbon nanotubes in CNT/epoxy-composites, Chemical Physics Letters 370/5-6 (2003) 820-824.

[114] W. Zhou, J. Vavro, N.M. Nemes, J.E. Fischer, F. Borondics, K. Kamarás, D.B. Tanner, Charge transfer and Fermi level shift in p-doped single-walled carbon nanotubes, Physical Review B 71 (2005) 205423.

[115] F. Beuneu, C.L. Huillier, J.P. Salvetat, J.M. Bonard, L. Forró, Modification of multiwall carbon nanotubes by electron irradiation, An ESR study, Physical Review B 59 (1999) 5945-5949.

[116] V. Zhirnov, D. Herr, M. Meyyappan, Electronic applications of carbon nanotubes become closer to reality, Journal of Nanoparticle Research 1 (1999) 151-152.

[117] A.S. Kotosonov, Texture and magnetic anisotropy of carbon nanotubes in cathode deposits obtained by the electric-arc method, JETP Letters 7 (1999) 476-480.

[118] A.S. Claye, N.M. Nemes, A. Jánossy, J.E. Fischer, Structure and electronic properties of potassium-doped single-wall carbon nanotubes, Physical Review B 62 (2000) R4845-R4848.

[119] J.P. Salvetat, T. Fehér, C. L'Huillier, F. Beuneu, L. Forró, Anomalous electron spin resonance behavior of single-walled carbon nanotubes, Physical Review B 72 (2005) 075440.

[120] P. Stamenov, J.M.D. Coey, Magnetic susceptibility of carbon-experiment and theory, Journal of Magnetism and Magnetic Materials 290-291 (2005) 279-285.

[121] S. Numao, S. Bandow, S. Iijima, Variable-range hopping conduction in the assembly of boron-doped multiwalled carbon nanotubes, The Journal of Physical Chemistry C 111/32 (2007) 11763-11766.

[122] M. Galambos, G. Fábiá, F. Simon, L. Ciric, L. Forró, L. Korecz, A. Rockenbauer, J. Koltai, V. Zólyomi, A. Rusznyák, J. Kürti, N. M. Nemes, B. Dóra, H. Peterlik, R. Pfeiffer, H. Kuzmany, T. Pichler, Identifying the electron spin resonance of conduction electrons in alkali doped SWCNTs, Physica Status Solidi B 246 (2009) 2760-2763.

[123] W. Schiessl, W. Potzel, H. Karze, M. Steiner, G.M. Kalvius, A. Martin, M.K. Krause, I. Halevy, J. Gal, W. Schafer, G. Will, M. Hillberg, R. Wappling, Magnetic properties of the ZnFe2O4 spinel, Physical Review B 53 (1996) 9143-9152.

[124] V. Sepelak, K. Tkacova, V.V. Boldyrev, S. Wissmann, K.D. Becker, Mechanically induced cation redistribution in ZnFe2O4 and its thermal stability, Physica B, Condensed Matter 234-236 (1997) 617-619.

[125] T.M. Clark, B.J. Evans, Enhanced magnetization and cation distributions in nanocrystalline ZnFe2O4, A conversion electron Mossbauer spectroscopic investigation, IEEE Transactions on Magnetics 33 (1997) 3745-3747.

[126] C.N. Chinnasamy, A. Narayanasamy, N. Ponpandian, K. Chattopadhyay, H. Guerault, J.-M. Greneche, Magnetic properties of nanostructured ferrimagnetic zinc ferrite, Journal of Physics, Condensed Matter 12 (2000) 7795-7805.

[127] C.N. Chinnasamy, A. Narayanasamy, N. Ponpandian, R. Joseyphus, Justin, K. Chattopadhyay, K. Shinoda, B. Jeyadevan, K. Tohji, K. Nakatsuka, J. M. Greneche, Ferrimagnetic ordering in nanostructured CdFe2O4 spinel, Journal of Applied Physics 90 (2001) 527-529.

[128] Y. Yamada, K. Kamazawa, Y. Tsunoda, Interspin interactions in ZnFe2O4: Theoretical analysis of neutron scattering study, Physical Review B 66 (2002) 064401-1-7.

[129] K. Kamazawa, Y. Tsunoda, H. Kadowaki, K. Kohn, Magnetic neutron scattering measurements on a single crystal of frustrated ZnFe2O4, Physical Review B 68 (2003) 024412-1-9.

[130] J.H. Shim, S. Lee, J.H. Park, S.-J. Han, Y.H. Jeong, Y.W. Cho, Coexistence of ferrimagnetic and antiferromagnetic ordering in Fe-inverted zinc ferrite investigated by NMR, Physical Review B 73 (2006) 064404-1-4.

[131] C. Cheng, Physical mechanism of extraordinary electromagnetic transmission in dual-metallic grating structures, Physical Review B 78 (2008) 075406-1-9.

[132] Y. Koseoglu, H. Yildiz, R. Yilgin, Synthesis, characterization and superparamagnetic resonance studies of $ZnFe_2O_4$ nanoparticles, Journal of Nanoscience and Nanotechnology 12 (2012) 2261-9.

[133] M. Sertkol, Y. Koseoglu, A. Baykal, H. Kavas, M.S. Toprak, Synthesis and magnetic characterization of $Zn_{0.7}Ni_{0.3}Fe_2O_4$ nanoparticles via microwave-assisted combustion route, Journal of Magnetism and Magnetic Materials 322/7 (2010) 866-871.

[134] M. Mozaffari, M. Eghbali Arani, J. Amighian, Preparation and investigation of magnetic properties of MnNiTi-substituted strontium hexaferrite nanoparticles, Journal of Magnetism and Magnetic Materials 322/18 (2010) 2670-2674.

[135] Z. Roslaniec, G. Broza, K. Schulte, Nanocomposites based on multiblock polyester elastomers (PEE) and carbon nanotubes (CNT), Composite Interfaces 10 (2003) 95-102.

[136] M. Kurzawa, A. Blonska-Tabero, I. Rychlowska-Himmel, P. Tabero, Reactivity of $FeVO_4$ towards oxides and pyrovanadates(V) of Co and Ni, Materials Research Bulletin 36 (2001) 1379-1390.

[137] M. Kurzawa, A. Blonska-Tabero, The synthesis and selected properties of new compounds: $Mg_3Fe_4(VO_4)_6$ and $Zn_3Fe_4(VO_4)_6)$, Materials Research Bulletin 36/7 (2002) 849.

[138] A. Biedunkiewicz, Crystallization of TiC and TiN from a colloidal system, Materials Science 21/4 (2003) 445-452.

[139] A. Biedunkiewicz, A. Strzelczak, G. Mozdzen, J. Lelatko, Non-isothermal oxidation of ceramic nanocomposites using the example of Ti-Si-C-N powder: Kinetic analysis method, Acta Materialia 56 (2008) 3132-3145.

[140] A.B. Bourlinos, E.P. Giannelis, Y. Sanakis, A. Bakandritsos, M. Karakassides, M. Gjoka, P. Petridis, A graphite oxide-like carbogenic material derived from a molecular precursor, Carbon 44 (2006) 1906-1912.

[141] M. Romcevic, R. Kostic, M. Romcevic, B. Hadzic, I. Kuryliszyn-Kudelska, W. Dobrowolski, U. Narkiewicz, D. Sibera, Raman scattering from ZnO(Fe) nanoparticles, Acta Physica Polonica A 114/5 (2008) 1323-1328.

[142] N. Guskos, J. Typek, M. Maryniak, Z. Roslaniec, D. Petridis, M. Kwiatkowska, FMR study of γ-Fe_2O_3 magnetic nanoparticles in a multiblock poly(ether-ester) copolymer matrix, Materials Science-Poland 23/4 (2005) 971-976.

[143] N. Guskos, M. Wabia, M. Kurzawa, A. Bezkrovnyj, J. Typek, I. Rychlowska-Himmel, A. Blonska-Tabero, Neutron diffraction study of $M_2FeV_3O_{11-\delta}$ compounds, Radiation Effects in Solids 158 (2003) 369-374.

[144] N. Guskos, J. Typek, A. Bezkrovnyj, V. Likodimos, M. Wabia, M. Kurzawa, E.A. Anagnostakis, G. Gasiorek, Neutron studies of cation disorder in $Zn_2FeV_3O_{11-\delta}$, Journal of Alloys and Compounds 377/1-2 (2004) 47-52.

[145] N. Guskos, A. Bezkrovnjj, J. Typek, N.Yu. Ryabova, A. Blonska-Tabero, M. Kurzawa, M. Maryniak, Neutron study of $Zn_3Fe_4V_6O_{24}$, Journal of Alloys and Compounds 391 (2005) 20.

[146] A. Bezkrovnyi, N. Guskos, J. Typek, N. Yu. Ryabova, M. Bosacka, A. Blonska-Tabero, M. Kurzawa, I. Rychlowska-Himmel, G. Zolnierkiewicz, Neutron diffraction study of $Mn_3Fe_4V_6O_{24}$, Materials Science-Poland 23/4 (2005) 883-890.

[147] A. Beskrovnyy, N. Guskos, J. Typek, N. Yu. Ryabova, A. Blonska-Tabero, M. Kurzawa, G. Zolnierkiewicz, Crystal structure of $Mg_3Fe_4V_6O_{24}$ studies by neutron diffraction, Reviews on Advanced Materials Science 11 (2006) 166.

[148] C.P. Poole, Electron spin resonance, Wiley-Interscience, New York, 1983.

[149] D.L. Huber, Critical-point anomalies in the electron-paramagnetic-resonance linewidth and in the zero-field relaxation time of antiferromagnets, Physical Review B 6 (1972) 3180-3186.

[150] C. Oliva, L. Formi, A.V. Vishniakov, Spin glass formation in $La_{0.9}Sr_{0.1}CoO_3$ catalyst for flameless combustion of methane, Spectrochimica acta A, Molecular and biomolecular spectroscopy 56 (2000) 301-307.

[151] N. Guskos, J. Typek, G. Zolnierkiewicz, R. Szymczak, P. Berczynski, K. Wardal, A. Blonska-Tabero, Magnetic properties of a new iron lead vanadate $Pb_2FeV_3O_{11}$ Journal of Alloys and Compounds 509 (2011) 8153-8157.

[152] N. Guskos, V. Likodimos, S. Glenis, J. Typek, J. Majszczyk, G. Zolnierkiewicz, A. Blonska-Tabero, C.L. Lin, Magnetic and dielectric study of $Ni_2FeV_3O_{11-\delta}$, Reviews on Advanced Materials Science 14 (2007) 14-34.

[153] L.V. Bershov, EPR spectra of $3d^n$ ions in beryl crystals, Zhurnal Structurnoy Khimii 10 (1969) 141.

[154] M. Sterrer, E. Fischbach, T. Risse, H.-J. Freund, Geometric characterization of a singly charged oxygen vacancy on a single-crystalline MgO(001) film by electron paramagnetic resonance spectroscopy, Physical Review Letters 94/18 (2005) 186101.

[155] S.V. Chong, K. Kadowaki, J. Xia, H. Idriss, Interesting magnetic behavior from reduced titanium dioxide nanobelts, Applied Physics Letters 92/23 (2008) 232502-232502-3.

[156] X. Wei, R. Skomski, B. Balamurugan, Z.G. Sun, S. Ducharme, D.J. Sellmyer, Magnetism of TiO and TiO_2 nanoclusters, Journal of Applied Physics 105/7 (2009) 07C517-1-3.

[157] N. Guskos, V. Likodimos, S. Glenis, G. Zolnierkiewicz, J. Typek, C.L. Lin, A. Biedunkiewicz, Magnetic properties of TiC_x/C nanocomposites, Journal of Non-crystalline Solids 354 (2008) 4330-4333.

[158] H.R. Zhang, H.W. Zheng, Y.Z. Gu. Y. Liang, Y.R. Cao, K.Q. Tan, TiC and TiN compounds, Proceedings of the 7th National Confrence on Functional Materials and Applications, China 1-3 (2010) 359.

[159] S. Yang, W. Tang, Y. Ishikawa, Q. Feng, Synthesis of titanium dioxide with oxygen vacancy and its visible-light sensitive photocatalytic activity, Materials Research Bulletin 46/4 (2011) 531-537.

[160] S. Numao, S. Bandow, S. Iijima, Control of the innermost tube diameters in multiwalled carbon nanotubes by the vaporization of boron-containing carbon rod in RF plasma, Journal of Physical Chemistry C 111 (2007) 4543-4548.

[161] J. Kliva, Electron Magnetic resonance of nanoparticles, Supermagnetic resonance in magnetic nanoparticles, S.P. Gubin (Ed.), Wiley-VCH, 2009, 255.